Sai Manikiran Garimella; Mohan Anand; Kumbakonam R. Rajagopal
A new model to describe the response of a class of seemingly viscoplastic materials

Applications of Mathematics, Vol. 67 (2022), No. 2, 153–165

Persistent URL: `http://dml.cz/dmlcz/149564`

A NEW MODEL TO DESCRIBE THE RESPONSE OF A CLASS OF SEEMINGLY VISCOPLASTIC MATERIALS

Sai Manikiran Garimella, Mohan Anand, Sangareddy,
Kumbakonam R. Rajagopal, College Station

Received July 13, 2020. Published online April 12, 2021.

Abstract. A new model is proposed to mimic the response of a class of seemingly viscoplastic materials. Using the proposed model, the steady, fully developed flow of the fluid is studied in a cylindrical pipe. The semi-inverse approach is applied to obtain an analytical solution for the velocity profile. The model is used to fit the shear-stress data of several supposedly viscoplastic materials reported in the literature. A numerical procedure is developed to solve the governing ODE and the procedure is validated by comparison with the analytical solution.

Keywords: viscoplastic fluid; constitutive model; pipe flow; semi-inverse method; exact solution

MSC 2020: 34B60

1. Introduction

The response of many materials, such as crude oil, drilling mud, mineral slurries, suspensions, paint, pastes, and meat extract are usually considered to be viscoplastic materials. These viscoplastic materials are used to describe applications in the fields of petroleum engineering, civil engineering, food processing, biophysics, meteorology, and hydraulic engineering. Numerous constitutive relations have been proposed to describe the response of viscoplastic materials, namely those due to Bingham [1], Herschel-Bulkley [6], Casson [4] and others. A detailed review of viscoplastic fluids can be found in Bird, Dai and Yarusso [2], Mitsoulis [8], and Huilgol [7]. The quintessential feature of such materials is that they seem to exhibit a "yield stress"

S. M. Garimella was supported by the MHRD Fellowship for Research Scholars administered by IIT Hyderabad.

DOI: 10.21136/AM.2021.0163-20

and then flow like a fluid. While these materials seem to exhibit a “yield stress” it is possible that this is a consequence of the experimental methodology as to how the fluid under question is subject to external stimuli, in this case the traction applied to the experimental apparatus. Whether indeed one has a material that exhibits a “yield stress” or flows with the application of shear stress, however small the shear stress might be, could be an artifice of the time scale and length scale of observation, and the extent of force applied[1].

We have referred to the constitutive relations developed by Bingham, Herschel-Bulkley, Casson and others as materials other than a “fluid” as we would like the term “fluid” to define the class of materials which are incapable of resisting shear stress and we would like to develop a constitutive relation that in some sense is “close” to capturing what seems to be observed in materials which are modeled as having a “yield stress”. The Queensland experiment described in the footnote suggests that if one just observed the experiment on asphalt for, say one hour, one might incorrectly conclude that the material in question has a “yield stress” as definitely even under the stress produced by gravity it does not seem to flow. However, such a conclusion would be incorrect for if the person waited long enough, the fluid would eventually flow just under the force of gravity. The viscosity of the fluid close to zero shear rate is so large and its resistance to flow is such that the shear rate is too small to be observed by the recording instrument, just our visual observation, in question. Thus, a fluid model that has an exceedingly high viscosity close to zero shear rate would be a reasonable approximation of the situation that is described by assuming a “yield stress”. The different viscoplastic materials such as the “Bingham fluid”, “Herschel-Bulkley fluid” and “Casson fluid” differ in the way they flow after the shear stress exceeds the “yield stress”. “The Bingham fluid” flows like a Navier-Stokes fluid once the shear stress exceeds the “yield stress”, while the others flow like power-law fluids. However, none of the above models are fluids in the sense that they are unable to resist shear. We are interested in developing a fluid constitutive relation and thus the model should have the ability to display an arbitrarily large slope with regard to the shear stress-shear rate curve and be able to capture the flow of the fluids under consideration. The materials that we want to describe, kaolin-water, meat extract and paint, seem to be reasonably well described by the constitutive relation that we consider. The constitutive relation is characterized by two constants, α_1 and α_2 (see

[1] Of course, it depends on the time of observation with regards to which the material does not seem to flow. It is possible if the observer were to wait a very long time the material might flow. In the classic experiment in Queensland (see [5]) on asphalt, it took as many as nine years for a drop of asphalt to fall. Thus, even if the observer had waited for one year it might have looked as though no flow was taking place. It also depends on the length scale of observation. If viewed under a tunneling electron microscope one might be able to detect movement which one cannot see with the naked eye.

the model (2.1)–(2.4)) with the shear stress τ tending to the asymptotic limit $\sqrt{2}\alpha_1$ as the shear rate κ increases, that is $\tau \to \sqrt{2}\alpha_1$ as $\kappa \to \infty$. Thus, the fluid is a limiting shear stress fluid. Moreover, the initial slope of the shear stress versus shear rate curve is $\frac{\mathrm{d}\tau}{\mathrm{d}\kappa}(0) = \alpha_1\alpha_2$, and thus we have flexibility to pick α_1 sufficiently large. The question is whether we can fit the experimental data, and our study shows that we can do so reasonably well. The model that we propose should only be considered as a first attempt at trying to approximate materials, that are described as materials with a "yield stress", by fluid models. It is possible to obtain better models with regard to predicting data by just adding one additional parameter as the two constants, that define our model, just fix the initial slope and the final asymptotic value.

Recently, Blechta et al. [3] have provided a thorough classification of incompressible fluids that span the gamut from Euler fluids, Navier-Stokes fluids, classical and stress power-law fluids, as well as fluids that have a variety of yield conditions that they refer to as activated fluids. Activated fluids are not fluids if one were to interpret fluids as we have done in this paper. The fluid under consideration here is a sub-class of a generalized Stokesian fluid and falls within the classification provided by Blechta et al. [3].

The fact that the material has "yield condition" makes the numerical study of general three dimensional problems most challenging. As observed earlier, we have an expression for the kinematics in terms of stress in the case of such fluids. In fact, such an approach is in keeping with the demands of causality (see [9]). However, one cannot substitute such an expression for the symmetric part of the velocity gradient in terms of the stress into the balance of linear momentum and get a partial differential equation for the velocity as in the case of the stress being expressed in terms of the symmetric part of the velocity gradient. Thus, the balance of linear momentum and the constitutive relation have to be solved simultaneously, and in the case of an incompressible fluid this leads to a system of ten unknowns (pressure, three components of the velocity and six components of the stress) and ten partial differential equations (conservation of mass that reduces to the constraint that the motion be isochoric, the balance of linear momentum and the six scalar constitutive relations relating the symmetric part of the velocity gradient and the stress). This is a very daunting task. In this paper, we develop a constitutive relation for the stress in terms of the velocity gradient. The stress can then be directly substituted into the balance of linear momentum to obtain a partial differential equation for the velocity, thereby simplifying the solution procedure for the problem. Of course, providing a constitutive relation for the stress goes against the demands of causality. The present work focuses on the flow features for a particular boundary value problem that has relevance to a problem of importance in engineering practice, namely steady fully-developed flow in a cylindrical pipe.

The paper is organized as follows. The new constitutive model is described in Section 2. The flow problem, namely steady fully developed flow in a cylindrical pipe, is introduced and the governing equations developed for the same in Section 3. An analytical solution is obtained by assuming a special form for the velocity field for the flow in an infinite straight cylindrical pipe in Section 4. The determination of the material parameters that describe the model, by comparison with experimental data, is carried out in Section 5, and the analytical solution and numerical solution are compared. We summarize the results and discuss future work in Section 6.

2. Constitutive model

We consider a constitutive relation for the Cauchy stress tensor $\mathbf{T}$ that is given by

$$\mathbf{T} = -p\mathbf{I} + 2\mu(\|\mathbf{D}\|)\mathbf{D}, \tag{2.1}$$

where

$$\mathbf{D} = \frac{1}{2}[\nabla\mathbf{v} + (\nabla\mathbf{v})^\top], \tag{2.2}$$

and

$$\|\mathbf{D}\| = \sqrt{\text{trace}(\mathbf{D}^2)}. \tag{2.3}$$

In (2.1)–(2.3), $-p\mathbf{I}$ is the indeterminate part of the stress due to the constraint of incompressibility (p is the mean value of the stress and is also the mechanical pressure, that is $(-\frac{1}{3})\,\text{trace}(\mathbf{T})$) and $\mu(\|\mathbf{D}\|)$ is the generalized viscosity which is dependent on the symmetric part of the velocity gradient $\mathbf{D}$, $\mathbf{v}$ denotes the velocity, and $\|\mathbf{D}\|$ is the Frobenius norm of the symmetric part of the velocity gradient.

We assume that $\mu(\|\mathbf{D}\|)$ is given by

$$\mu(\|\mathbf{D}\|) = \frac{\alpha_1}{\|\mathbf{D}\|} - \frac{\alpha_1 \exp(-\alpha_2\|\mathbf{D}\|)}{\|\mathbf{D}\|}, \tag{2.4}$$

where α_1 and α_2 are positive constants. Unlike the constitutive relations for viscoplasticity, our proposed constitutive relation does not exhibit a “yield stress”. Moreover, when a shear stress is applied, however small it might be, the body described by the constitutive relation will flow. With regard to a real material, as mentioned earlier, whether it flows or not might depend on the time scale of observation, and thus it is far from clear whether the materials that are currently described by the viscoplastic constitutive model do truly exhibit a “yield stress”. Our belief is that the proposed model holds promise as an alternative to a class of viscoplastic materials, especially those that seem to exhibit an asymptotic value for the stress as the shear rate increases. We verify that this is indeed the case by comparison with experimental data.

3. Problem formulation

We consider the fluid defined by (2.1)–(2.4) flowing in a cylindrical pipe. The flow is assumed to be steady, axisymmetric, and fully developed. The schematic of the flow domain with the coordinates marked is given in Figure 1.

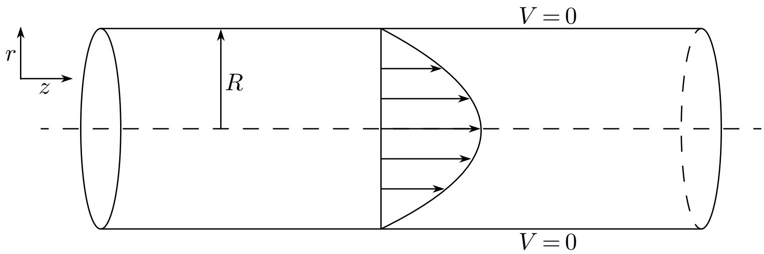

Figure 1. Schematic representation of fully developed flow in a cylindrical pipe.

The balance equations of mass and linear momentum are given by

$$\frac{\partial \varrho}{\partial t} + \operatorname{div}(\varrho \mathbf{v}) = 0, \tag{3.1}$$

$$\operatorname{div} \mathbf{T} + \varrho \boldsymbol{b} = \varrho \frac{\mathrm{D}\mathbf{v}}{\mathrm{D}t}, \tag{3.2}$$

where $\partial/\partial t$ is the partial derivative with respect to time, ϱ is the density of the fluid, $\operatorname{div}(\cdot)$ denotes the divergence operator, and $\mathbf{v} = v_r \mathbf{e}_r + v_\theta \mathbf{e}_\theta + v_z \mathbf{e}_z$ is the velocity vector with the components of the velocity in the directions r, θ, and z as v_r, v_θ, and v_z, respectively. Further, $\boldsymbol{b}$ is the body force, and $\mathrm{D}(\cdot)/\mathrm{D}t$ is the Lagrangian time derivative, which is given by $\partial(\cdot)/\partial t + \operatorname{grad}(\cdot)\mathbf{v}$.

In the cylindrical polar coordinate system, (3.1)–(3.2) can be expressed as given below.

Mass balance equation:

$$\frac{\partial \varrho}{\partial t} + \frac{1}{r}\frac{\partial}{\partial r}(\varrho r v_r) + \frac{1}{r}\frac{\partial}{\partial \theta}(\varrho v_\theta) + \frac{\partial}{\partial z}(\varrho v_z) = 0. \tag{3.3}$$

Momentum balance equation in each coordinate direction is given below:

In the r-coordinate direction:

$$\varrho\Big(\frac{\partial v_r}{\partial t} + v_r\frac{\partial v_r}{\partial r} + \frac{v_\theta}{r}\frac{\partial v_r}{\partial \theta} + v_z\frac{\partial v_r}{\partial z} - \frac{v_\theta^2}{r}\Big) = \Big[\frac{1}{r}\frac{\partial}{\partial r}(r\tau_{rr}) + \frac{1}{r}\frac{\partial}{\partial \theta}(\tau_{\theta r}) + \frac{\partial}{\partial z}(\tau_{zr}) - \frac{\tau_{\theta\theta}}{r}\Big] - \frac{\partial p}{\partial r} + \varrho g_r, \tag{3.4}$$

In the θ-coordinate direction:

$$\varrho\Big(\frac{\partial v_\theta}{\partial t} + v_r\frac{\partial v_\theta}{\partial r} + \frac{v_\theta}{r}\frac{\partial v_\theta}{\partial \theta} + v_z\frac{\partial v_\theta}{\partial z} + \frac{v_r v_\theta}{r}\Big) = \Big[\frac{1}{r^2}\frac{\partial}{\partial r}(r^2\tau_{r\theta}) + \frac{1}{r}\frac{\partial}{\partial \theta}(\tau_{\theta\theta}) + \frac{\partial}{\partial z}(\tau_{z\theta})\Big] + \Big[\frac{\tau_{\theta r} - \tau_{r\theta}}{r}\Big] - \frac{1}{r}\frac{\partial p}{\partial \theta} + \varrho g_\theta, \tag{3.5}$$

In the z-coordinate direction:

$$\varrho\Big(\frac{\partial v_z}{\partial t} + v_r\frac{\partial v_z}{\partial r} + \frac{v_\theta}{r}\frac{\partial v_z}{\partial \theta} + v_z\frac{\partial v_z}{\partial z}\Big) = \Big[\frac{1}{r}\frac{\partial}{\partial r}(r\tau_{rz}) + \frac{1}{r}\frac{\partial}{\partial \theta}(\tau_{\theta z}) + \frac{\partial}{\partial z}(\tau_{zz})\Big] - \frac{\partial p}{\partial z} + \varrho g_z. \tag{3.6}$$

4. Analytical solution

We use a semi-inverse method for solving the problem analytically for steady, fully developed flow in a cylindrical pipe geometry.

We assume the velocity field and the pressure field are of the form

$$\mathbf{v} = v_z(r)\mathbf{e}_z, \quad p = p(r, z), \tag{4.1}$$

i.e., the flow is in z-direction and $\mathbf{e}_z$ denotes the unit vector in the z-coordinate direction.

Using the assumed flow field and neglecting gravity, (3.4)–(3.6) simplify to

$$-\frac{\partial p}{\partial r} = 0, \tag{4.2}$$

$$-\frac{1}{r}\frac{\partial p}{\partial \theta} = 0, \tag{4.3}$$

$$\frac{1}{r}\frac{\partial}{\partial r}(r\tau_{rz}) - \frac{\partial p}{\partial z} = 0. \tag{4.4}$$

The boundary condition for the velocity is

$$\text{no-slip condition: } v_z = 0 \text{ at } r = R. \tag{4.5}$$

We augment the boundary condition with a symmetry condition, namely,

$$\text{symmetry condition: } \frac{\mathrm{d}v_z}{\mathrm{d}r} = 0 \text{ at } r = 0. \tag{4.6}$$

The governing equations for the flow for the proposed constitutive relation are obtained by substituting the simplified Cauchy stress tensor into (4.2), (4.3), (4.4).

For the assumed flow field, the symmetric part of the velocity gradient $\mathbf{D}$ simplifies to

$$\mathbf{D} = \frac{1}{2}\begin{bmatrix} 0 & 0 & \frac{\mathrm{d}v_z}{\mathrm{d}r} \\ 0 & 0 & 0 \\ \frac{\mathrm{d}v_z}{\mathrm{d}r} & 0 & 0 \end{bmatrix}. \tag{4.7}$$

Subsequently, for the assumed flow field, the Cauchy stress tensor (2.1) is expressed as

$$\mathbf{T} = \begin{bmatrix} -p & 0 & \mu(\|\mathbf{D}\|)\frac{\mathrm{d}v_z}{\mathrm{d}r} \\ 0 & -p & 0 \\ \mu(\|\mathbf{D}\|)\frac{\mathrm{d}v_z}{\mathrm{d}r} & 0 & -p \end{bmatrix}. \tag{4.8}$$

Thus

$$\tau_{rz} = \mu(\|\mathbf{D}\|)\frac{\mathrm{d}v_z}{\mathrm{d}r}. \tag{4.9}$$

In order to describe the solution characteristics clearly, the governing equations are non-dimensionalized and the solution is expressed in terms of dimensionless variables. The dimensionless quantities that are used in this procedure are

$$p^* = \frac{pR}{\mu_0 u_0}, \quad z^* = \frac{z}{R}, \quad r^* = \frac{r}{R}, \quad \alpha_1^* = \frac{\alpha_1 R}{\mu_0 u_0},$$
$$\alpha_2^* = \frac{\alpha_2 u_0}{R}, \quad v_z^* = \frac{v_z}{u_0}, \quad \mu^*(\|\mathbf{D}\|) = \frac{\mu(\|\mathbf{D}\|)}{\mu_0},$$

where R is the radius of the pipe, μ_0 is the reference viscosity, and u_0 is the reference velocity.

In terms of dimensionless variables, the equations (4.2)–(4.4) are written as

$$-\frac{\partial p^*}{\partial r^*} = 0, \tag{4.10}$$

$$-\frac{1}{r^*}\frac{\partial p^*}{\partial \theta^*} = 0, \tag{4.11}$$

$$\frac{1}{r^*}\frac{\partial}{\partial r^*}(r^* \tau_{rz}^*) - \frac{\partial p^*}{\partial z^*} = 0. \tag{4.12}$$

In terms of dimensionless variables, (4.5)–(4.6) are expressed as

$$v_z^* = 0 \text{ at } r^* = 1, \tag{4.13}$$

$$\frac{\mathrm{d}v_z^*}{\mathrm{d}r^*} = 0 \text{ at } r^* = 0. \tag{4.14}$$

From (4.10)–(4.11), we note that the pressure is a function of z only. This, taken along with (4.12), implies that $\mathrm{d}p^*/\mathrm{d}z^* =$ constant. Upon integration, (4.12) leads to

$$\tau_{rz}^* = \left(\frac{\mathrm{d}p^*}{\mathrm{d}z^*}\right)\frac{r^*}{2} + \frac{c_1}{r^*}, \tag{4.15}$$

where $\mathrm{d}p^*/\mathrm{d}z^*$ is a constant and c_1 is the integration constant.

At $r^* = 0$, τ_{rz}^* is finite, which implies that $c_1 = 0$. Hence, (4.15) simplifies to

$$\tau_{rz}^* = \left(\frac{\mathrm{d}p^*}{\mathrm{d}z^*}\right)\frac{r^*}{2}. \tag{4.16}$$

In terms of the dimensionless form, (4.9) is expressed as

$$\tau_{rz}^* = \mu^*(\|\mathbf{D}\|)\frac{\mathrm{d}v_z^*}{\mathrm{d}r^*}. \tag{4.17}$$

From (2.2) and (2.3),

$$\|\mathbf{D}\| = \sqrt{\mathrm{trace}(\mathbf{D}^2)} = \frac{1}{\sqrt{2}}\left|\frac{\mathrm{d}v_z}{\mathrm{d}r}\right| = \frac{1}{\sqrt{2}}\frac{u_0}{R}\left|\frac{\mathrm{d}v_z^*}{\mathrm{d}r^*}\right|. \tag{4.18}$$

Now, by equating (4.16) and (4.17), we get

$$\left(\frac{\mathrm{d}p^*}{\mathrm{d}z^*}\right)\frac{r^*}{2} = \mu^*(\|\mathbf{D}\|)\frac{\mathrm{d}v_z^*}{\mathrm{d}r^*}. \tag{4.19}$$

By substituting (2.4), (4.18) in (4.19), we obtain

$$\left(\frac{\mathrm{d}p^*}{\mathrm{d}z^*}\right)\frac{r^*}{2} = \left[-\sqrt{2}\alpha_1^* + \sqrt{2}\alpha_1^* \exp\left(-\alpha_2^*\frac{1}{\sqrt{2}}\left|\frac{\mathrm{d}v_z^*}{\mathrm{d}r^*}\right|\right)\right], \tag{4.20}$$

which, as α_1^* is assumed to be non-zero, can be rearranged as

$$1 + \frac{1}{2\sqrt{2}\alpha_1^*}\left(\frac{\mathrm{d}p^*}{\mathrm{d}z^*}\right)r^* = \exp\left(-\alpha_2^*\frac{1}{\sqrt{2}}\left|\frac{\mathrm{d}v_z^*}{\mathrm{d}r^*}\right|\right). \tag{4.21}$$

Applying the natural logarithm on both sides, we obtain

$$\ln\Big(1+\frac{1}{2\sqrt{2}\alpha_1^*}\Big(\frac{\mathrm{d}p^*}{\mathrm{d}z^*}\Big)r^*\Big) = -\alpha_2^*\frac{1}{\sqrt{2}}\Big|\frac{\mathrm{d}v_z^*}{\mathrm{d}r^*}\Big|, \tag{4.22}$$

$$\Big|\frac{\mathrm{d}v_z^*}{\mathrm{d}r^*}\Big| = -\frac{\mathrm{d}v_z^*}{\mathrm{d}r^*} = -\frac{\sqrt{2}}{\alpha_2^*}\ln\Big(1+\frac{1}{2\sqrt{2}\alpha_1^*}\Big(\frac{\mathrm{d}p^*}{\mathrm{d}z^*}\Big)r^*\Big), \tag{4.23}$$

$$v_z^* = \frac{\sqrt{2}}{\alpha_2^*}\Big(\int \ln\Big(1+\frac{1}{2\sqrt{2}\alpha_1^*}\Big(\frac{\mathrm{d}p^*}{\mathrm{d}z^*}\Big)r^*\Big)\,\mathrm{d}r^*\Big) + k. \tag{4.24}$$

Equation (4.24) gets simplified (with the application of integration by parts) to

$$v_z^* = \frac{1}{\alpha_2^*}\ln\Big(1+\frac{1}{2\sqrt{2}\alpha_1^*}\Big(\frac{\mathrm{d}p^*}{\mathrm{d}z^*}\Big)r^*\Big)\Big[\sqrt{2}r^* + \frac{4\alpha_1^*}{\mathrm{d}p^*/\mathrm{d}z^*}\Big] - \frac{\sqrt{2}r^*}{\alpha_2^*} + k. \tag{4.25}$$

The boundary and symmetry conditions are applied to (4.25) to obtain the final velocity profile, which is expressed as

$$\begin{aligned} v_z^* = {} & \frac{\sqrt{2}}{\alpha_2^*}\ln\Big(1+\frac{1}{2\sqrt{2}\alpha_1^*}\Big(\frac{\mathrm{d}p^*}{\mathrm{d}z^*}\Big)\Big)\Bigg[-1+\frac{r^*\ln\Big(1+\frac{(\mathrm{d}p^*/\mathrm{d}z^*)r^*}{2\sqrt{2}\alpha_1^*}\Big)}{\ln\Big(1+\frac{\mathrm{d}p^*/\mathrm{d}z^*}{2\sqrt{2}\alpha_1^*}\Big)}\Bigg] \\ & + \frac{4\alpha_1^*}{(\mathrm{d}p^*/\mathrm{d}z^*)\alpha_2^*}\ln\Bigg[\frac{1+\frac{(\mathrm{d}p^*/\mathrm{d}z^*)r^*}{2\sqrt{2}\alpha_1^*}}{1+\frac{\mathrm{d}p^*/\mathrm{d}z^*}{2\sqrt{2}\alpha_1^*}}\Bigg] + \frac{\sqrt{2}}{\alpha_2^*}(1-r^*). \end{aligned} \tag{4.26}$$

5. Model corroboration and comparison

In this section, the parameters α_1 and α_2, that define the proposed model (given in (2.1)–(2.4)) are determined by corroborating against experimental data using MATLAB 2018a. We fit the proposed model with the experimental data for shear-stress versus shear-rate reported in the literature. We then compare the analytical and numerical solutions for the proposed model.

The expression for the generalized viscosity $\mu(\|\mathbf{D}\|)$ is determined by (2.4) and the norm of the symmetric part of the velocity gradient $\mathbf{D}$ is determined by

$$\|\mathbf{D}\| = \frac{1}{\sqrt{2}}\frac{\mathrm{d}v_z}{\mathrm{d}r}.$$

We obtain the non-linear equation for $\mu(\|\mathbf{D}\|)$ to be solved at each value, in terms of $\mathrm{d}v_z/\,\mathrm{d}r$:

$$\mu(\|\mathbf{D}\|) = \frac{\sqrt{2}\alpha_1}{\mathrm{d}v_z/\mathrm{d}r} - \frac{\sqrt{2}\alpha_1\exp(-\frac{\alpha_2}{\sqrt{2}}(\mathrm{d}v_z/\mathrm{d}r))}{\mathrm{d}v_z/\mathrm{d}r}. \tag{5.1}$$

The equation for the absolute shear stress (for given $\mathrm{d}v_z/\mathrm{d}r$) is thus

$$\tau_{rz} = \sqrt{2}\alpha_1 - \sqrt{2}\alpha_1 \exp\Big(-\frac{\alpha_2}{\sqrt{2}}\frac{\mathrm{d}v_z}{\mathrm{d}r}\Big). \tag{5.2}$$

The experimental data for the (absolute value) shear stress versus shear rate are reported for kaolin-water suspension, meat extract and paint in [2] and [8], respec-

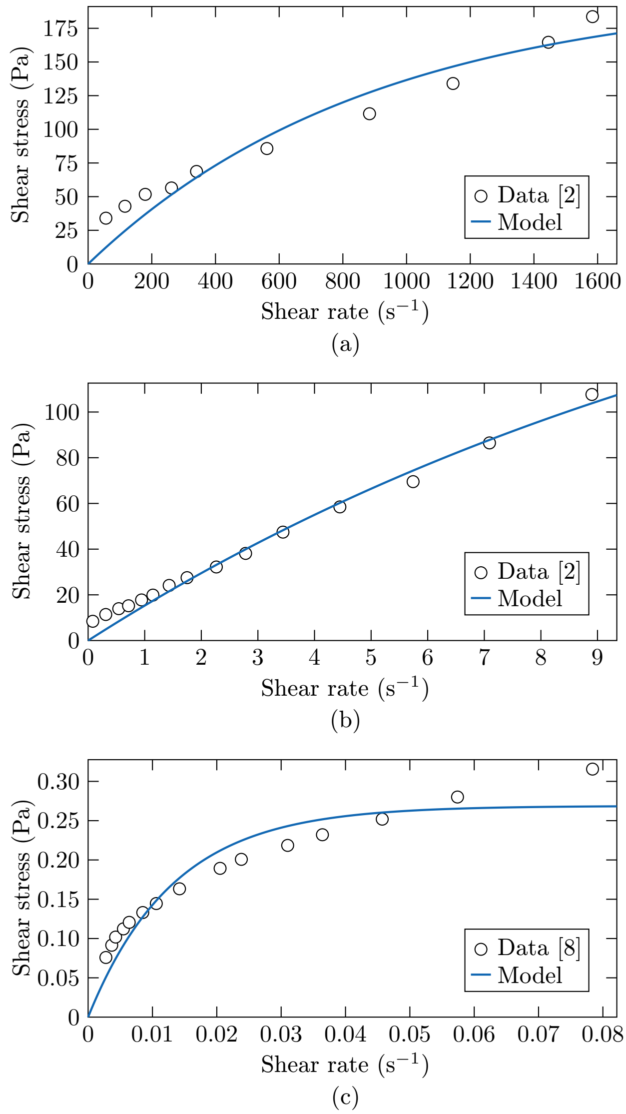

Figure 2. Shear stress as a function of shear rate fitted to experimental data for (a) kaolin-water [2], (b) meat extract [2], and (c) paint [8].

tively. We use the above expression for the shear stress and corroborate against experimental data at the same shear rate. The curve fitting tool (cftool) in MATLAB 2018a is used to determine α_1 and α_2 for the best fit. The agreement of the predictions of the model with data for the selected fluids is shown in Figures 2(a)–(c). However, we can claim that the model is effective only if we can corroborate data for a totally different experiment with the same values for the material constants, and this will be a part of our future work. The constants obtained are (for kaolin-water: $\alpha_1 = 1.44 \times 10^2\,\mathrm{N/m^2}$, $\alpha_2 = 1.58 \times 10^{-3}\,\mathrm{s}$), (for meat extract: $\alpha_1 = 1.54 \times 10^2\,\mathrm{N/m^2}$, $\alpha_2 = 1.03 \times 10^{-1}\,\mathrm{s}$), and (for paint: $\alpha_1 = 1.90 \times 10^{-1}\,\mathrm{N/m^2}$, $\alpha_2 = 1.07 \times 10^2\,\mathrm{s}$), respectively. The fitted model is a smooth function for the shear stress in terms of the shear rate that ensures that the fluid will flow, however small the shear stress.

5.1. Comparison of the exact solution and the numerical solution for the model. We test our numerical solution against the predictions of the analytical solution to make sure that the numerical procedure is not incorrect. The non-linear (non-dimensional) second-order ODE

$$\frac{\mathrm{d}^2 v_z^*}{\mathrm{d}r^{*2}} = \frac{1}{\alpha_1^* \alpha_2^*}\left(\frac{\mathrm{d}p^*}{\mathrm{d}z^*} + \frac{\sqrt{2}\alpha_1^*}{r^*}\right)\exp\left(-\frac{\alpha_2^*}{\sqrt{2}}\frac{\mathrm{d}v_z^*}{\mathrm{d}r^*}\right) - \frac{\sqrt{2}}{r^*\alpha_2^*} \tag{5.3}$$

is solved numerically and its validity tested against the analytical solution defined earlier. The above ordinary differential equation is solved subject to no-slip and symmetry boundary conditions. The numerical method given below is used to solve the equation governing steady fully developed flow in a pipe.

The numerical method uses subroutines ode45 and fsolve of MATLAB, and implements the shooting method. This reduces the boundary value problem to an initial value problem as mentioned below. In this method the second-order ODE is converted to a system of two first-order ODEs. We solve for $\mathrm{d}^2 v_z^*/\mathrm{d}r^{*2}$ at each radius (r) that satisfies the above equation and the symmetry condition ($\mathrm{d}v_z^*/\mathrm{d}r^* = 0$). The iteration proceeds until the velocity at the pipe wall tends to zero. With the help of input parameters (α_1^* and α_2^* for the fluid model that has been proposed, obtained from fitting experimental data, and the pressure gradient $\mathrm{d}p^*/\mathrm{d}z^*$), the equation is solved iteratively and the velocity profiles are constructed. The programs are coded in MATLAB R2018a software and executed on an Intel-Xeon 2.30 GHz workstation (Model Fujitsu R-920).

The numerical procedure is validated by comparing the solution with the analytical solution: see Figure 3. We observe that the velocity profiles generated numerically match exactly with the analytical solution.

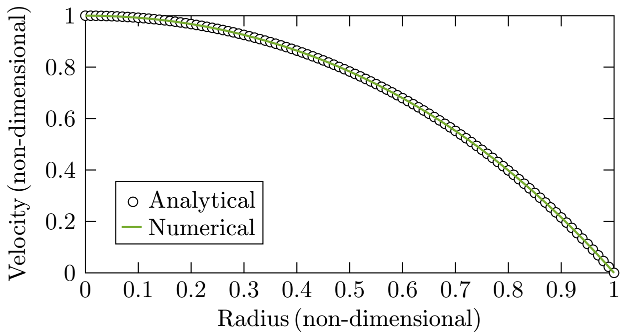

(a)

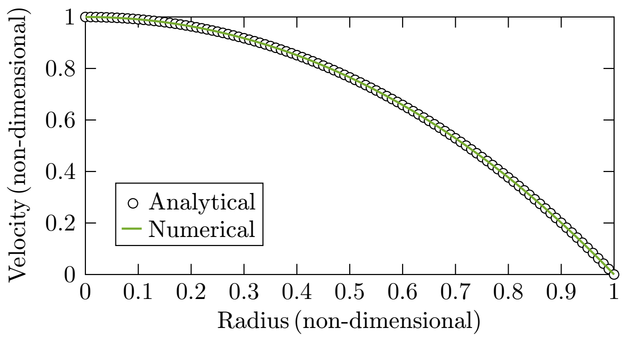

(b)

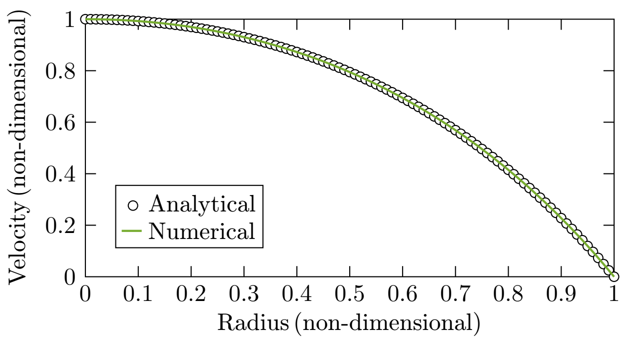

(c)

Figure 3. Fully developed velocity profiles of fluids in a cylindrical pipe flow of radius 0.1 m for (a) kaolin-water [2], (b) meat extract [2], and (c) paint [8].

6. Conclusion

We have developed a new model as an alternative for a class of viscoplastic models (that is, models that exhibit a yield stress). We have studied the flow behavior of the proposed model for the boundary value problem (BVP) of steady fully developed flow in a cylindrical pipe. The (non-dimensional) governing equation is solved analytically with the help of the semi-inverse approach and the velocity profile is obtained. We chose material parameters for our model that fitted the shear stress data reported for real fluids. In order to determine the predictive capability of the above model, we have to use the material parameters that we have used to fit the data and corroborate against a new set of experiments. This will be a part of our future work. We developed a numerical method to solve the ODE equation governing the BVP and the solution compared well against the analytical solution thus validating the numerical method.

The advantages of the proposed model are that it is consistent with the definition of a fluid, in the body under consideration cannot resist shear stresses, and allows for a smooth variation of viscosity from zero shear rate onwards. In future work, we will study the model for other flow problems, and also consider modifications to the model so that we can obtain a better description of the response of the bodies under consideration.

References

[1] *E. C. Bingham*: Fluidity and Plasticity. McGraw-Hill, New York, 1922.

[2] *R. B. Bird, G. C. Dai, B. J. Yarusso*: The rheology and flow of viscoplastic materials. Rev. Chem. Eng. *1* (1983), 1–70. doi

[3] *J. Blechta, J. Málek, K. R. Rajagopal*: On the classification of incompressible fluids and a mathematical analysis of the equations that govern their motion. SIAM J. Math. Anal. *52* (2020), 1232–1289. zbl MR doi

[4] *N. Casson*: A flow equation for pigment-oil suspensions of the printing ink type. Rheology of Disperse Systems. Pergamon Press, Oxford, 1959, pp. 84–104. zbl

[5] *R. Edgeworth, B. J. Dalton, U. T. Parnell*: The pitch drop experiment. Eur. J. Phys. *5* (1984), 198–200. doi

[6] *W. H. Herschel, R. Bulkley*: Konsistenzmessungen von Gummi-Benzollösungen. Kolloid-Z. *39* (1926), 291–300. (In German.) doi

[7] *R. R. Huilgol*: Fluid Mechanics of Viscoplasticity. Springer, Berlin, 2015. zbl doi

[8] *E. Mitsoulis*: Flows of viscoplastic materials: Models and computations. Rheology Rev. *2007* (2007), 135–178.

[9] *K. R. Rajagopal*: Conspectus of concepts of elasticity. Math. Mech. Solids *16* (2011), 536–562. zbl MR doi

Authors' addresses: *Sai Manikiran Garimella*, *Mohan Anand* (corresponding author), Department of Chemical Engineering, Indian Institute of Technology Hyderabad, Sangareddy, Telangana 502285, India, e-mail: `anandm@che.iith.ac.in`; *Kumbakonam R. Rajagopal*, Department of Mechanical Engineering, Texas A&M University, College Station, TX 77843, USA, e-mail: `krajagopal@tamu.edu`.